AGU PUBLICATIONS

Geophysical Research Letters

RESEARCH LETTER
10.1002/2015GL065378

Key Points:
- Upper ocean cooling due to winds of Hurricane Gonzalo was small
- Mixing-induced cooling partially suppressed by near-surface stratification due to salinity
- Ocean response to Hurricane Gonzalo involved multiple upper ocean processes

Supporting Information:
- Text S1 and Figure S1

Correspondence to:
R. Domingues,
Ricardo.Domingues@noaa.gov

Citation:
Domingues, R., G. Goni, F. Bringas, S.-K. Lee, H.-S. Kim, G. Halliwell, J. Dong, J. Morell, and L. Pomales (2015), Upper ocean response to Hurricane Gonzalo (2014): Salinity effects revealed by targeted and sustained underwater glider observations, *Geophys. Res. Lett.*, *42*, 7131–7138, doi:10.1002/2015GL065378.

Received 14 JUL 2015
Accepted 7 AUG 2015
Accepted article online 11 AUG 2015
Published online 4 SEP 2015

Upper ocean response to Hurricane Gonzalo (2014): Salinity effects revealed by targeted and sustained underwater glider observations

Ricardo Domingues[1,2], Gustavo Goni[2], Francis Bringas[2], Sang-Ki Lee[1,2], Hyun-Sook Kim[3,4], George Halliwell[2], Jili Dong[1,2,4], Julio Morell[5,6], and Luis Pomales[5]

[1]Cooperative Institute for Marine and Atmospheric Studies, University of Miami, Miami, Florida, USA, [2]Atlantic Oceanographic and Meteorological Laboratory, NOAA/OAR, Miami, Florida, USA, [3]I. M. Systems Group Inc., and Marine Modeling and Analysis Branch, College Park, Maryland, USA, [4]Environmental Modeling Center, NOAA/NWS, College Park, Maryland, USA, [5]University of Puerto Rico Mayaguez, Mayaguez, Puerto Rico, [6]Caribbean Coastal Observing System, CariCOOS, Lajas, Puerto Rico

Abstract During October 2014, Hurricane Gonzalo traveled within 85 km from the location of an underwater glider situated north of Puerto Rico. Observations collected before, during, and after the passage of this hurricane were analyzed to improve our understanding of the upper ocean response to hurricane winds. The main finding in this study is that salinity potentially played an important role on changes observed in the upper ocean; a near-surface barrier layer likely suppressed the hurricane-induced upper ocean cooling, leading to smaller than expected temperature changes. Poststorm observations also revealed a partial recovery of the ocean to prestorm conditions 11 days after the hurricane. Comparison with a coupled ocean-atmosphere hurricane model indicates that model-observations discrepancies are largely linked to salinity effects described. Results presented in this study emphasize the value of underwater glider observations for improving our knowledge of how the ocean responds to tropical cyclone winds and for tropical cyclone intensification studies and forecasts.

1. Introduction

The study of ocean processes forced by the passage of a tropical cyclone (TC) is critical for understanding air-sea interactions that can lead to the intensification of TCs and, therefore, for improving models used for hurricane prediction. For example, the presence of large upper ocean heat content [*Shay et al.,* 2000; *Lin et al.,* 2008; *Mainelli et al.,* 2008; *Goni et al.,* 2015] and barrier layers [*Balaguru et al.,* 2012a] (i.e., increased salinity stratification near the surface) can effectively reduce storm-induced sea surface temperature (SST) cooling, favoring the intensification of the TC. Previous studies showed that the upper ocean response to TCs is dominated by the development of vertical mixing, upwelling on the wake of the hurricane, and baroclinic processes [*Price et al.,* 1994; *Dickey et al.,* 1998; *Prasad and Hogan*, 2007]. Most of these studies were based on modeling outputs, on satellite data alone, or on very limited in situ data, such as Argo floats, moored instruments, or Airborne eXpendable BathyThermographs. In this study, we used underwater glider observations that were geared exclusively toward providing targeted in situ ocean observations to investigate the ocean environment under hurricane force winds.

In July 2014, two underwater gliders (hereafter referred to as gliders) were deployed off Puerto Rico as part of a multiinstitutional effort. The two gliders were piloted along predetermined tracks in the Caribbean Sea and in the North Atlantic Ocean (Figure 1), where hurricanes very often travel and intensify [e.g., *Landsea*, 1993]. During July through November 2014, both gliders continuously provided temperature and salinity profile data to 1000 m and depth-averaged and surface current velocities.

On 12 October 2014, TC Gonzalo developed in the tropical North Atlantic, intensifying into Category 1 hurricane (17.9°N, 62.9°W) on 13 October and into Categories 2 (19.1°N, 64.0°W) and 3 (20.8°N, 65.6°W) on 14 October. At that stage, Hurricane Gonzalo had a well-defined eye with diameter of ~29 km and maximum sustained winds of 100 knots (~51 m/s) [*Stewart*, 2014]. During its intensification into Category 3, Hurricane Gonzalo traveled ~85 km northeast of the location of the glider (Figure 1), providing an exceptional opportunity to collect upper ocean observations under hurricane wind conditions. The sampling strategy adopted

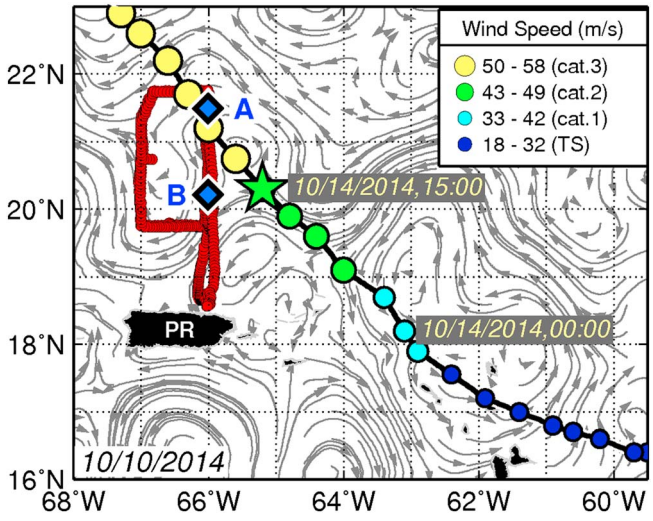

Figure 1. Track followed by the glider (red points) north of Puerto Rico (PR) during July–November 2014, overlaid on altimetry-derived geostrophic currents. During 8–28 October, the glider sampled ocean conditions between sites A and B (blue diamonds). The track of Hurricane Gonzalo is shown by colored circles (every 3 h). The star highlights the closest location of the hurricane with respect to the glider.

during the passage of Hurricane Gonzalo consisted of carrying out observations: along a repeat section 3 times, one before and two after the passage of the hurricane, and at a fixed location during the passage of the hurricane.

The goal of this work is to help improve the understanding of the upper ocean response to hurricane force winds. To accomplish this we assess ocean conditions before (prestorm), during, and after (poststorm) the passage of Hurricane Gonzalo along a transect north of Puerto Rico (Figure 1); quantify the observed upper ocean variability; and discuss potential mechanisms associated with the observed upper ocean changes. Glider observations were further compared with outputs from a numerical coupled atmospheric-ocean model used for hurricane prediction to evaluate the model performance in simulating the upper ocean response during Hurricane Gonzalo.

2. Ocean Observations

Here, ocean conditions were assessed based on 228 temperature and salinity profiles collected by the glider during the period of 8–28 October 2014 along 66°W between 20°N and 21.5°N (meridional section $\overline{AB}$; Figure 1), focusing on the following: prestorm and poststorm temperature conditions along section $\overline{AB}$; and time series of temperature and salinity anomalies at site B during the passage of Hurricane Gonzalo. All temperature and salinity profiles analyzed in this study were quality controlled based on gross-range tests, spike detection, vertical gradients checks, and comparison to climatological temperature and salinity conditions from the World Ocean Atlas 2013 [*Locarnini et al.,* 2013; *Zweng et al.,* 2013].

2.1. Prestorm Observations

During the prestorm period of observations (8–15 October 2014), this glider obtained 54 temperature and salinity profiles while traveling along section $\overline{AB}$ outside the outer boundary of a cyclonic feature (Figure 1). The prestorm temperature section (Figure 2a) showed that there was an upper layer with homogenous temperature of ~29°C above 50 m. The base of this layer corresponded to the depth of the seasonal thermocline, which was characterized by a large vertical gradient (0.1°C/m) in temperature below 50 m (Figure 3a).

On 13 October, the glider arrived at site B. The temperature profile at this location had characteristics similar to the profiles observed between sites A and B (Figure 3a). It was estimated that prestorm temperature conditions had a high upper ocean heat content (sometimes referred as Tropical Cyclone Heat Potential, TCHP [*Goni et al.,* 2009]) of 86 kJ/cm^2, which has been shown to play a key role in TC intensity changes [*Mainelli et al.,* 2008; *Lin et al.,* 2013], and also to affect the TC induced upper ocean cooling [*Lin et al.,* 2008]. Salinity observations at this location showed a shallow low-salinity layer above 20 m, with sea surface salinity (SSS) of 35.8 on 13 October (Figure 3b). The sharp increase in salinity between 10 and 20 m determined a strong vertical density gradient (~−0.032 kg/m^3/m) that characterized a barrier layer, which is generally defined as a layer of water separating the well-mixed surface layer from the thermocline [e.g., *Sprintall and Tomczak*, 1992; *Vissa et al.,* 2013]. Between 20 and 130 m, the salinity exhibited increasing values until it reached its highest value of 37.2 at 130 m.

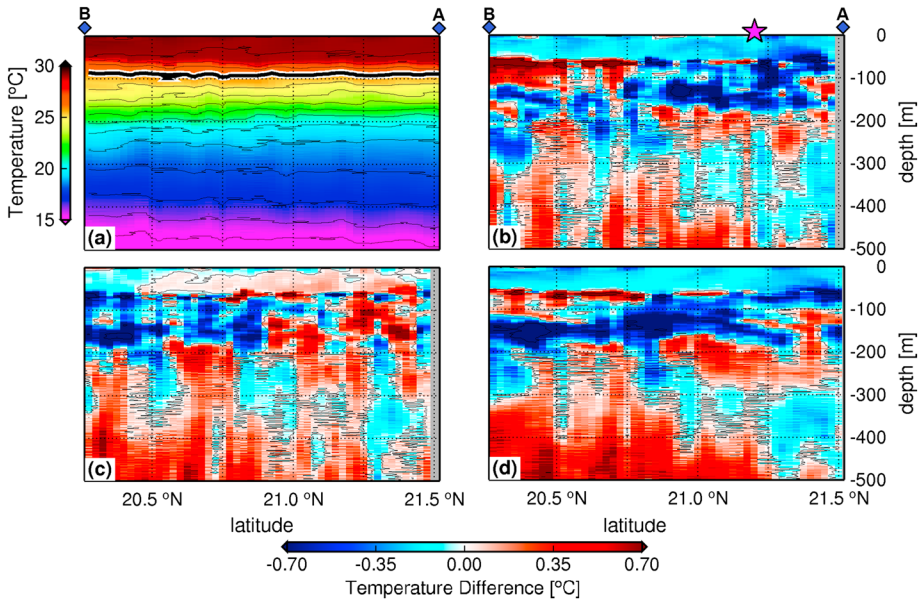

Figure 2. (a) Prestorm temperature along section $\overline{AB}$. Temperature differences between (b) first poststorm section and prestorm section; (c) second poststorm section and first poststorm section; and (d) second poststorm section and prestorm section. The star in Figure 2b identifies the latitude where Hurricane Gonzalo crossed section $\overline{AB}$.

2.2. During Storm Observations

During 13–15 October 2014, the glider was parked at site B (20.2°N, 66.0°W) and configured to sample every ~2 h (total of 28 profiles) to assess changes in ocean conditions at this location during the passage of Hurricane Gonzalo. During this 2 day record, Hurricane Gonzalo traveled from 16.6°N, 59.7°W to 22.6°N, 67.0°W (Figure 1). Site B was ~85 km southwest from the closest location of Hurricane Gonzalo on 15:00 UTC 14 October.

The 2 day record of temperature and salinity anomalies with respect to the initial conditions to 500 m at site B (Figures 3c and 3d) showed that the ocean exhibited different behavior in the upper and lower layers. Above 50 m (depth of the seasonal thermocline), temperature anomalies were mostly negative during the record (Figure 3c). These negative anomalies resulted from two main cooling events on 07:00 UTC 13 October and 14:00 UTC 14 October (not shown). Below 50 m, temperature anomalies were dominated by alternating positive and negative values. Observations also showed that larger salinity anomalies occurred above 130 m (depth of the salinity maximum) (Figure 3d). Above 130 m, salinity anomalies were mostly negative, except in the layer between 0 and 20 m. Similar to temperature, alternating positive and negative salinity anomalies were observed below 130 m. Here temperature and salinity anomalies exhibited a significant positive correlation of 0.90 (95% confidence level) below 130 m, showing the coupled behavior of these parameters.

To further assess the dominant modes of variability that occurred in the upper ocean at site B during the 2 day record, density anomalies were decomposed into sets of Empirical Orthogonal Functions (EOFs, depth dependent) and of principal components (PCs, time dependent). Approximately 85% of the observed variability in the density structure at site B was accounted by three modes. The first mode (red line, Figures 3e and 3f) characterized density anomalies confined to the upper ~130 m with opposite signs above and below 20 m and explained 38% of the density variability. The second mode (green line, Figures 3e and 3f) characterized density anomalies with opposite signs above and below 100 m and explained 31% of the density variability. The third mode (blue line, Figures 3e and 3f) showed two changes in sign, one at ~20 m and the other at ~50 m, and explained 16% of the density variability. The observed sign changes at ~20 m for the first and third modes indicate that the low salinity layer above 20 m played an important role in the density structure at site B. In addition, the first PC time series showed increasing values during the 2 day record (red line, Figure 3f), reaching its peak value on 20:00 UTC 14 October, 5 h after Hurricane Gonzalo traveled the closest from the glider. The PC time series for the second and third modes exhibited an alternating pattern (green and blue lines, Figure 3f), indicating periodic changes in the vertical structure of the density field.

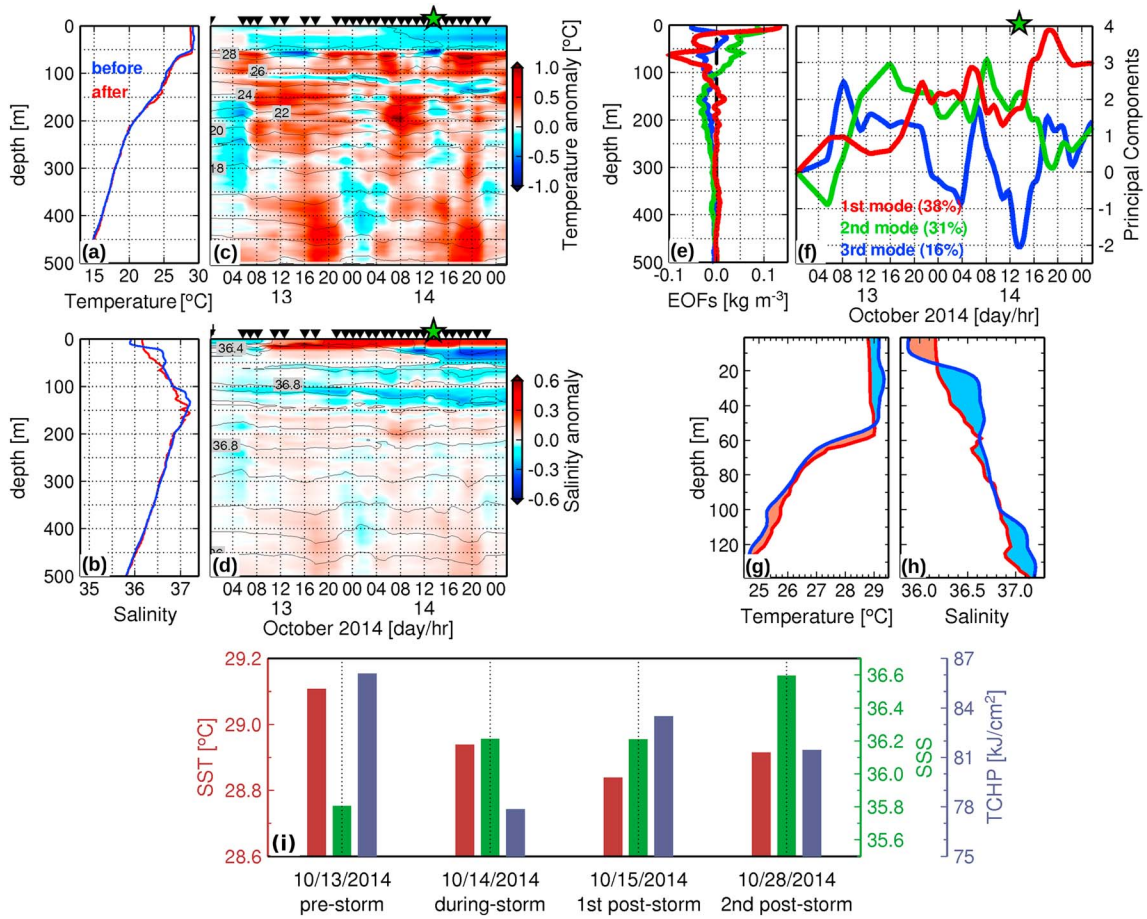

Figure 3. (a) Prestorm (blue line) and poststorm (red line) temperature profiles at site B. (b) Same as Figure 3a but for salinity. (c) Depth-time diagram of temperature anomalies during the 2 day record at site B. (d) Same as Figure 3c but for salinity. (e) EOFs and (f) principal components of density anomalies at site B. (g) and (h) shows in detail Figures 3a and 3b, respectively, for the depth range between 0 and 130 m. (i) Summary of upper ocean conditions observed at site B during the study period. The green star on Figures 3c, 3d, and 3f indicates the time when Hurricane Gonzalo was the closest from site B.

2.3. Poststorm Observations

In order to investigate the ocean response after the passage of Hurricane Gonzalo, section $\overline{AB}$ was repeated two additional times: from site B to site A, during 15–23 October (first poststorm section, 94 profiles), and from site A to site B, during 23–28 October (second poststorm section, 52 profiles). Temperature observations were interpolated into a regular grid of 1 m depth per 0.025° of latitude and compared with the pre storm section (Figure 2a) described in section 2.1.

Temperature differences between the first poststorm section and the prestorm section (Figure 2b) showed a well-defined colder layer above 50 m. This upper layer was, in average, 0.4°C colder than prestorm conditions, with values as low as −1°C in the proximity of site A, which was located slightly to the north (right) of Hurricane Gonzalo's track (Figure 1). In general, negative temperature differences were mostly observed in the northern part of the section (between 20.8°N and 21.5°N), occupying most of the water column in the proximity of site A.

Temperature differences between the second and the first poststorm sections (Figure 2c) indicated that the upper ocean started to warm 11 days after the passage of the hurricane. This warming was evidenced by positive temperature differences (~0.1°C) found above 50 m along section $\overline{AB}$. Temperature differences between the second poststorm section and the prestorm section (Figure 2d) showed that 11 days after the storm, the upper 50 m was still 0.3°C colder than prestorm conditions. The colder temperatures in the northern part of the section (20.8°N–21.5°N) also persisted for a period longer than 11 days. Figure 3i provides a summary of observed upper ocean changes at site B.

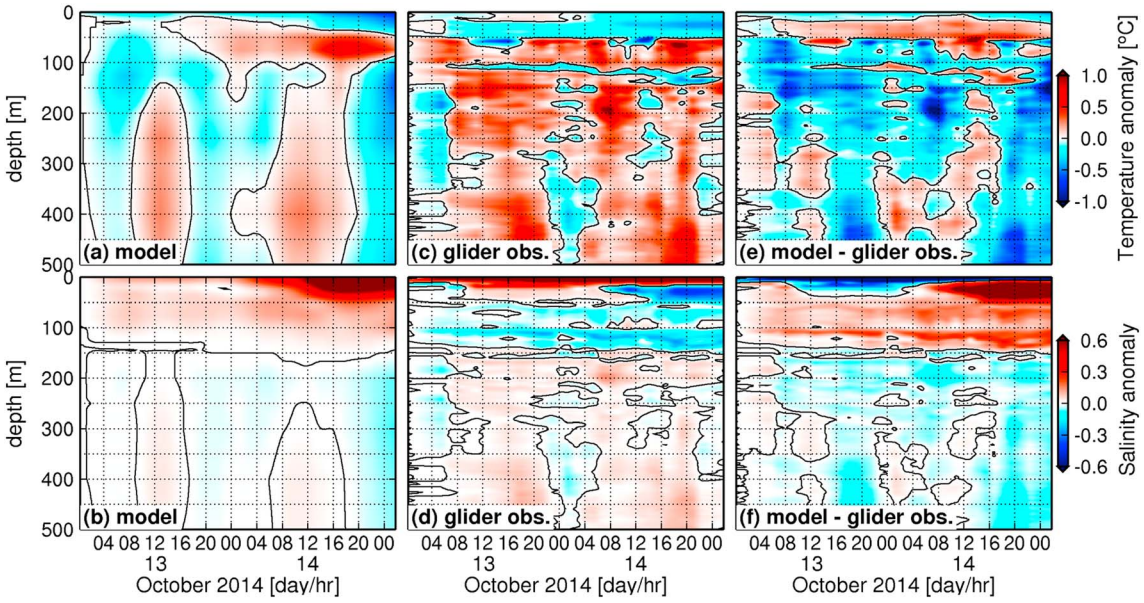

Figure 4. (a) Depth-time diagrams of model-derived temperature anomalies from HYCOM-HWRF during a 2 day time series at site B. (b) Same as Figure 4a but for model-derived salinity. (c) Same as Figure 3c. (d) Same as Figure 3d. (e and f) The difference between model-derived and observed (glider) temperature and salinity anomalies at site B, respectively.

3. Modeling Results

Glider observations were further compared with real-time oceanic simulations conducted using the coupled HYbrid Coordinate Ocean Model (HYCOM) to the Hurricane Weather Research Forecast model (HWRF), HYCOM-HWRF [e.g., *Kim et al.,* 2014]. Numerical model outputs of temperature and salinity at site B during the same 2 day record exhibited good qualitative agreement with glider observations, showing the following: an overall cooling of the upper 50 m (Figure 4a), which was also the depth of the seasonal thermocline in the model; warming between 50 and 100 m; alternating positive and negative temperature (Figure 4a) and salinity (Figure 4b) anomalies below 130 m; and an increase in salinity above 130 m (Figure 4b), which also corresponded to the depth of the salinity maximum in the model.

Differences between model-derived and glider-derived temperature and salinity anomalies at site B indicated that the model overestimated (underestimated) the cooling at the surface cooling (between 20 and 50 m) by 0.2°C (Figure 4e) and that model-derived salinity anomalies exhibited large differences (up to 1) with respect to glider observations (Figure 4f). These differences may be partially due to the following: (a) the underestimated wind speeds of the hurricane by HWRF (24 knot, or ~12 m/s, of average intensity error); (b) hurricane track errors in the model forecast (28 nm of average track error in the area of analysis); and (c) discrepancies in initial conditions for salinity. Salinity is, in general, an ocean parameter less accurately reproduced by the model used here, which is partially due to the scarcity of salinity observations assimilated into the model. This is an important issue, given that regions off Puerto Rico are sensitive to different freshwater sources, such as the Amazon and Orinoco rivers [*Kelly et al.,* 2000; *Corredor et al.,* 2003; *Balaguru et al.,* 2012a; *Johns et al.,* 2014]. The assimilation of precipitation and fresh water sources in the model as well as the improvement in vertical discretization may enable a better representation of salinity features, such as the shallow low-salinity layer observed above 20 m.

4. Discussion

Glider observations analyzed in this study showed a complex response of the upper ocean, which may be caused by the influence of multiple processes linked with hurricane forced winds. Observations collected at site B during the storm (13–15 October) indicated that different processes may have dominated the variability in the layer above 130 m and in the layer between 130 and 500 m. Above 130 m, the observed temperature and salinity anomalies were uncorrelated and were consistent with the effect of mixing, which has been

identified as the main process leading to upper ocean cooling due to TC activity [*Price*, 1981; *Prasad and Hogan*, 2007]. Because of the characteristics of the initial temperature and salinity profiles at site B (Figures 3a and 3b), vertical mixing in the layer above 130 m would cause a decrease in temperature (anomalies of −0.4°C) above 50 m and an increase in temperature (anomalies of 0.4°C) between 50 and 130 m (Figure 3g). Likewise, mixing would cause an increase in salinity above 20 m (anomalies of 0.6) and a decrease in salinity below this depth (anomalies of −0.4) (Figure 3h). The changes observed above 130 m were consistent with wind-forced mixing, which were captured by the first mode of the density variability in this location that accounted for 38% of the total variability (red lines, Figure 3e). This mode showed a maximum value 5 h after Hurricane Gonzalo traveled closest to site B (green star, Figure 3f), indicating the time when the largest temperature and salinity anomalies were observed above 130 m. This 5 h delay is consistent with the time frame of the *forced stage*, characterized as the period of intense mixing when the ocean is directly under the influence of TC winds [*Price et al.,* 1994]. Therefore, one main result from this study is that during the passage of Hurricane Gonzalo, observed changes in ocean conditions above 130 m were likely linked with wind-forced mixing, causing 38% of the density variability at site B.

While changes in ocean conditions above 130 m were likely dominated by wind-driven mixing mechanisms at site B, the correlation ($r = 0.90$, significant at the 95% confidence level based on a Student's t test) between temperature and salinity anomalies between 130 and 500 m indicated the occurrence of periodic vertical displacements of isopycnal surfaces, possibly linked with internal tides and baroclinic processes. This is supported by the periodic changes in density revealed by the second and third modes of variability (Figures 3e and 3f). For example, the second PC time series showed low values with an approximate 20 h time difference (green line, Figure 3f). This time difference was consistent with the effect of near-inertial oscillations, considering that the inertial period at site B (20.20°N) is 35 h. Peak-to-peak changes in the third PC showed a 12–24 h time difference (blue line, Figure 3f), consistent with semidiurnal and diurnal tidal components at this location. Therefore, we can conclude that ~47% of the density variability in the upper 500 m at site B was likely linked with background motions due to internal tides and near-inertial baroclinic motions partly forced by the storm. This 2 day record allowed the detection of periodic background signals in addition to the largest changes directly produced by the hurricane winds. Longer ocean observational records in future targeted observations will enable the separation of the baroclinic signals induced directly by hurricane forced winds. This is important because baroclinic motions, such as the propagation of internal waves in the thermocline, are one of the means for dispersing the energy introduced by hurricane winds [*Brink*, 1989]. These motions are linked with the *inertial pumping effect*, which may drive vertical displacement of isotherms by values as large as 60 m to 70 m, similar to the values observed here, and that often last longer than 9 days [*Dickey et al.,* 1998].

Temperature observations collected along section $\overline{AB}$ 5 days after the passage of Hurricane Gonzalo (Figure 2b) showed an average cooling of −0.4°C mostly above 50 m in the proximity of site B, while stronger cooling of ~−1°C was observed in most of the water column in the proximity of site A, except for between 100 and 200 m. The cooling observed in the proximity of site B is consistent with the wind-driven mixing mechanism described above. The stronger cooling observed in the proximity of site A may be linked with two additional processes: wind-driven rightward biased cooling and intensified upwelling in the vicinity of the track of the hurricane. The primary reason for the rightward biased cooling is because of resonant winds and mixed-layer velocities on the right side of the storm, which produces a cooling pattern displaced to the right [*Price*, 1981]. While the rightward bias is generally associated with fast moving (>4 m/s) TCs [e.g., *Price et al.,* 1994; *Dickey et al.,* 1998; *Walker et al.,* 2005], upwelling usually has a more important role in slow moving storms (<4 m/s) [*Price*, 1981]. Storm-induced upwelling is driven by surface divergences in the wake of the storm [*Sanford et al.,* 1987], which produces an overall cooling of the water column similar to the temperature differences observed in the proximity of site A. Because Hurricane Gonzalo was a moderately fast moving (~5.2 m/s) TC during 13–15 October, it is likely that stronger cooling anomalies observed close to site A were caused by the two processes described above.

One important result from this study is that the observed upper ocean cooling observed during the passage of Hurricane Gonzalo was relatively small (between −0.4°C and −1°C) compared with cooling reported for other Atlantic hurricanes. For example, previous studies reported cooling anomalies with values of −3.5°C to −4°C during Hurricane Felix (1995) [*Dickey et al.,* 1998]; −2°C to −3°C during Hurricane Opal (1995)

[*Shay et al.,* 2000]; and −3°C to −7°C during Hurricane Ivan (2004) [*Walker et al.,* 2005]. Satellite observations showed that stronger cooling of −2°C due to the winds of Hurricane Gonzalo was only observed when it reached maximum intensity as a Category 4 hurricane at 23.5°N–68.0°W [*Goni et al.,* 2015].

One main finding of this study was that salinity played an important role in the upper ocean response to the winds of Hurricane Gonzalo. Prestorm conditions at site B were marked by the presence of a shallow low-salinity layer above 20 m (Figure 3b) that was associated with the presence of a barrier layer, which has potentially suppressed the upper ocean cooling due to Hurricane Gonzalo. To verify this hypothesis, the Richardson Number (Ri) above 50 m was computed for the 2 day record obtained at site B during the passage of the hurricane (Text S1 in the supporting information). Necessary and sufficient condition for occurrence of turbulent mixing requires Ri to be smaller than 0.25 for linear systems [*Miles*, 1961] and smaller than unity for nonlinear systems [*Abarbanel et al.,* 1984]. Estimates of Ri indicate that prestorm conditions were dominated by stratification effects due to salinity, with Ri equal to ~3. This value is approximately 2 orders of magnitude larger than the Ri estimated for homogenous salinity conditions above 50 m (~0.04). The large value of Ri during prestorm conditions observed at site B indicated that turbulent mixing was unlikely to occur due to strong stratification near the surface. Time series of the Ri above 50 m at site B (Figure S1) further indicated that the strong stratification near the surface was slowly eroded during the 2 day record. Values smaller than unity were only reached when Hurricane Gonzalo traveled the closest from site B on 14:00 UTC 14 October, which coincided with the strongest cooling event observed at this location. These results indicate that the barrier layer linked with prestorm salinity conditions near the surface has potentially reduced the mixing-induced cooling driven by Hurricane Gonzalo. In fact, previous studies [e.g., *Grodsky et al.,* 2012; *Balaguru et al.,* 2012b] also showed that salinity-induced barrier layers linked with the Amazon/Orinoco river plume could reduce the upper ocean cooling due to hurricanes. Our results provide additional evidence that salinity can efficiently affect the upper ocean cooling due to hurricane force winds. Similar salinity effects can be also observed in other ocean basins where fresh water sources affect upper ocean conditions, such as in the Indian Ocean [e.g., *Vissa et al.,* 2013]. Even though stratification effects may have largely suppressed the upper ocean cooling in the wake of Hurricane Gonzalo, it is also recognized here that the cooling may have also been partially restrained by the relatively high upper ocean heat content (86 kJ/cm^2) in the region [see *Lin et al.,* 2008]. In addition, Hurricane Gonzalo was less intense than other TCs analyzed by the studies described above, even though stronger cooling (−1.1°C) was also observed under weaker hurricane conditions of Josephine (1984, Category 2) [*Sanford et al.,* 1987].

Another important result revealed by the glider observations is that 11 days after the passage of Hurricane Gonzalo, the upper ocean started warming above 50 m (Figure 2c), but it did not fully recover to prestorm temperature conditions (Figure 2d). Numerical model outputs show that warming of the upper layers after the passage of a hurricane is mostly driven by horizontal advection [*Prasad and Hogan*, 2007], indicating the important role of the background ocean circulation. Further study and longer records of repeated sections will be needed to fully understand the role of the ocean dynamics and heat fluxes in the recovery processes. Regarding the model-observations discrepancies described in section 3, a better model representation of salinity conditions may improve simulations of the ocean response and future hurricane forecasts in this region, given the important role of salinity suggested by observations analyzed in this study.

Results presented here show the critical value of targeted and sustained glider observations. The observations analyzed in this study are part of those obtained by a network of underwater gliders that was implemented specifically in support of hurricane studies. For the first time, gliders were used to obtain ocean observations at a fixed location during the passage of one Atlantic hurricane and along a repeat section 3 times to assess upper ocean changes and recovery after the hurricane. Similar observations are expected to be performed during the following hurricane seasons. Future studies within this project will address in detail the impact of glider observations on hurricane forecasts.

Acknowledgments

This work was supported by the Disaster Relief Appropriations Act of 2013 (P.L. 113-2), also known as the Sandy Supplemental, through the NOAA research grant NA14OAR4830103, by NOAA's Atlantic Oceanographic and Meteorological Laboratory, and by CariCOOS (Caribbean Coastal Observing System). This research was also carried out under the auspices of the Cooperative Institute for Marine and Atmospheric Studies (CIMAS), University of Miami. The authors would like to thank the following members of the glider project, Grant Rawson (CIMAS), Walt McCall and Richard Bouchard (NOAA/NDBC), the crew from R/V *La Sultana* from UPRM, and Kongsberg for making this effort possible. The authors also thank Joaquin Trinanes for assistance with AVISO data sets, and Silvia Garzoli, Elisabeth Johns, and two reviewers for their insightful comments during final versions of this manuscript. Underwater glider data are made freely available by NOAA/AOML (available at: www.aoml.noaa.gov/phod/gliders) and by NOAA/IOOS (available at: http://data.ioos.us/gliders/providers/). The altimetry SSH products were produced by Ssalto/Duacs, distributed by AVISO, and supported by the CNES (available at: http://www.aviso.oceanobs.com/).

The Editor thanks M.M. Ali and Naresh Krishnavissa for their assistance in evaluating this paper.

References

Abarbanel, H. D., D. D. Holm, J. E. Marsden, and T. Ratiu (1984), Richardson number criterion for the nonlinear stability of three-dimensional stratified flow, *Phys. Rev. Lett.*, *52*(26), 2352.

Balaguru, K., P. Chang, R. Saravanan, and C. J. Jang (2012a), The barrier layer of the Atlantic warm pool: Formation mechanism and influence on the mean climate, *Tellus, Ser. A*, *64*, 18162.

Balaguru, K., P. Chang, R. Saravanan, L. R. Leung, Z. Xu, M. Li, and J. S. Hsieh (2012b), Ocean barrier layers' effect on tropical cyclone intensification, *Proc. Natl. Acad. Sci. U.S.A.*, *109*(36), 14,343–14,347.

Brink, K. H. (1989), Observations of the response of thermocline currents to a hurricane, *J. Phys. Oceanogr.*, *19*(7), 1017–1022.

Corredor, J., J. Morell, J. López, R. Armstrong, A. Dieppa, C. Cabanillas, A. Cabrera, and V. Hensley (2003), Remote continental forcing of phytoplankton biogeochemistry: Observations across the "Caribbean-Atlantic front", *Geophys. Res. Lett.*, *30*(20), 2057, doi:10.1029/2003GL018193.

Dickey, T., D. Frye, J. McNeil, D. Manov, N. Nelson, D. Sigurdson, H. Jannasch, D. Siegel, T. Michaels, and R. Johnson (1998), Upper-ocean temperature response to Hurricane Felix as measured by the Bermuda testbed mooring, *Mon. Weather Rev.*, *126*(5), 1195–1201.

Goni, G., et al. (2009), Applications of satellite-derived ocean measurements to tropical cyclone intensity forecasting, *Oceanography*, *22*(3).

Goni, G., J. A. Knaff, and I.-I. Lin (2015), State of the climate in 2014, *Bull. Am. Meteorol. Soc.*, *96*(7), S121–S122.

Grodsky, S. A., N. Reul, G. Lagerloef, G. Reverdin, J. A. Carton, B. Chapron, Y. Quilfen, V. N. Kudryavtsev, and H.-Y. Kao (2012), Haline hurricane wake in the Amazon/Orinoco plume: AQUARIUS/SACD and SMOS observations, *Geophys. Res. Lett.*, *39*, L20603, doi:10.1029/2012GL053335.

Johns, E. M., B. A. Muhling, R. C. Perez, F. E. Müller-Karger, N. Melo, R. H. Smith, J. T. Lamkin, T. L. Gerard, and E. Malca (2014), Amazon River water in the northeastern Caribbean Sea and its effect on larval reef fish assemblages during April 2009, *Fish. Oceanogr.*, *23*(6), 472–494.

Kelly, P. S., K. M. Lwiza, R. K. Cowen, and G. J. Goni (2000), Low-salinity pools at Barbados, West Indies: Their origin, frequency, and variability, *J. Geophys. Res.*, *105*(C8), 19,699–19,708, doi:10.1029/1999JC900328.

Kim, H.-S., C. Lozano, V. Tallapragada, D. Iredell, D. Sheinin, H. L. Tolman, V. M. Gerald, and J. Sims (2014), Performance of ocean simulations in the coupled HWRF-HYCOM model, *J. Atmos. Oceanic Technol.*, *2*, 545–559.

Landsea, C. W. (1993), A climatology of intense (or major) Atlantic hurricanes, *Mon. Weather Rev.*, *121*(6), 1703–1713.

Lin, I. I., C. C. Wu, I. F. Pun, and D. S. Ko (2008), Upper-ocean thermal structure and the western North Pacific Category 5 typhoons. Part I: Ocean features and the Category 5 typhoons' intensification, *Mon. Weather Rev.*, *136*(9), 3288–3306.

Lin, I. I., G. J. Goni, J. A. Knaff, C. Forbes, and M. M. Ali (2013), Ocean heat content for tropical cyclone intensity forecasting and its impact on storm surge, *Nat. Hazards*, *66*(3), 1481–1500.

Locarnini, R. A., et al. (2013), *World Ocean Atlas 2013*, *Temp., NOAA Atlas NESDIS 73*, vol. 1, edited by S. Levitus and A. Mishonov, 40 pp., NOAA, Silver Spring, Md.

Mainelli, M., M. DeMaria, L. Shay, and G. Goni (2008), Application of oceanic heat content estimation to operational forecasting of recent Atlantic Category 5 hurricanes, *Weather Forecasting*, *23*(1), 3–16.

Miles, J. W. (1961), On the stability of heterogeneous shear flows, *J. Fluid Mech.*, *10*(04), 496–508.

Prasad, T. G., and P. J. Hogan (2007), Upper-ocean response to Hurricane Ivan in a 1/25 nested Gulf of Mexico HYCOM, *J. Geophys. Res.*, *112*, C04013, doi:10.1029/2006JC003695.

Price, J. F. (1981), Upper-ocean response to a hurricane, *J. Phys. Oceanogr.*, *11*(2), 153–175.

Price, J. F., T. B. Sanford, and G. Z. Forristall (1994), Forced stage response to a moving hurricane, *J. Phys. Oceanogr.*, *24*(2), 233–260.

Sanford, T. B., P. G. Black, J. R. Haustein, J. W. Feeney, G. Z. Forristall, and J. F. Price (1987), Ocean response to a hurricane. Part I: Observations, *J. Phys. Oceanogr.*, *17*(11), 2065–2083.

Shay, L. K., G. J. Goni, and P. G. Black (2000), Effects of a warm oceanic feature on Hurricane Opal, *Mon. Weather Rev.*, *128*(5), 1366–1383.

Sprintall, J., and M. Tomczak (1992), Evidence of the barrier layer in the surface layer of the tropics, *J. Geophys. Res.*, *97*(C5), 7305–7316, doi:10.1029/92JC00407.

Stewart, S. R. (2014), Hurricane Gonzalo discussion number 10, National Hurricane Center, NOAA, Miami, Fla. [Available at http://www.nhc.noaa.gov/archive/2014/al08/al082014.discus.010.shtml, Accessed on July 30, 2014].

Vissa, N. K., A. N. V. Satyanarayana, and B. P. Kumar (2013), Response of upper ocean and impact of barrier layer on Sidr cyclone induced sea surface cooling, *Ocean Sci. J.*, *48*(3), 279–288.

Walker, N. D., R. R. Leben, and S. Balasubramanian (2005), Hurricane-forced upwelling and chlorophyll a enhancement within cold-core cyclones in the Gulf of Mexico, *Geophys. Res. Lett.*, *32*, L18610, doi:10.1029/2005GL023716.

Zweng, M. M., et al. (2013), *World Ocean Atlas 2013*, *Salinity, NOAA Atlas NESDIS 74*, vol. 2, edited by S. Levitus and A. Mishonov, 39 pp., NOAA, Silver Spring, Md.